Review Article

Asymmetry as an indicator of stress: From population statistics to clinical life-saving applications

Alex Frid[1] and Shmuel Raz[2]*

[1]Asher Space Research Institute, Technion, Israel

[2]Department of Information Systems, University of Haifa, Haifa 31905, Israel

Check for updates

Abstract

Most symmetrical objects can be efficiently described in terms of their deviation from a specific symmetry group, whether it be a mirror, radial, or translatory symmetry, among other groups. Fundamentally, asymmetry is an individual trait, but the asymmetry distribution of a given population may provide valuable information about the well-being of that population. Quantification of these deviations from perfect symmetry evolved from counts and linear measures of distances to landmarks conducive to structures with consistent topology, and then to Continuous Symmetry Measures (CSM) conducive to structures with no consistent topology. We demonstrate the usefulness of this approach on quantification of leaf veins that mirror bifurcating structures.

Deviations from a given symmetry group can be described in terms of (i) Fluctuating Asymmetries (FA) or (ii) broken asymmetries. Fluctuating Asymmetry (FA) is a controversial indicator of stress, and therefore tackling the problem needs a large number of species and populations in habitats with well-known stressors. We found such a site at "Evolution Canyon", Israel, and we examine and discuss a study of twenty-four species that live in the canyon's opposing slopes.

We conclude with examples from asymmetry as a neurophysiological bioindicator by presenting several studies on Amyotrophic Lateral Sclerosis (ALS), Parkinson's disease, and stroke. We show how machine-learning methods, applied on asymmetry indicators (in addition to the traditional signal processing features), can improve the sensitivity of the system and provide reliable diagnostic results.

Introduction

Symmetry is a quality of most objects in the universe, from molecules of hydrogen to galaxies, and across phylogeny, from bacteria to humans. Bilateral, radial, rotational, dihedral, and translational symmetries are present everywhere. These symmetries, however, are never perfect. Deviations from symmetry at the population level may be distributed (in the statistical sense) normally or leptokurtically around a mean of zero (Fluctuating Asymmetry, FA), around a mean different from zero (Directional Asymmetry, DA), or they may display platykurtic or bimodal distributions around a mean of zero (antisymmetry).

Fluctuating Asymmetry (FA) is a measure of developmental noise (random developmental variation) and developmental instability [1-3]. The study of fluctuating asymmetry began with bilateral structures [1-5] and it currently includes diverse symmetries (e.g., radial, translational, complex symmetry, etc.).

The basic measure of fluctuating asymmetry is the variance (or other measure of dispersion) of the studied feature on right and left sides of the symmetry axis, var (r – l), where *r* is the measure or count on the right side and *l* is the measure or count on the left side [3,5]. This approach, however, ignores the shape of a structure, and only considers linear distances of morphometric traits or counts of meristic traits. The use of landmarks and continuous symmetry measures enables us to have better insight by taking into account the shape of the structure [6-10].

Fluctuating asymmetry as an indicator of stress at the population level

Fluctuating asymmetry can serve as an indicator of

environmental and genetic stress [6,11-17], though its sensitivity is a debatable one [18,19]. The results of fluctuating asymmetry studies are inconsistent-sometimes it increases under environmental and genetic stress [20,21], and at other times it does not [22-24]

Linear asymmetry as a bio-indicator of stress-a microcosm of life's evolution at evolution canyon: Linear morphometric distances (e.g., distance from the symmetry axis), randomized sampling, and measurements applied to many species from a variety of taxa that share the same habitat, can be used to more precisely evaluate environmental stress and developmental instability [25,26]. We found such an appropriate environment in the Evolution Canyon microsites, where hundreds of studies have been conducted in the last 30 years [27-32] (Figure 1). The opposite slopes of Evolution Canyon are referred to as the "African" south-facing slope and the "European" north-facing slope, and they provide a wonderful opportunity for studying developmental instability in a natural experiment. The opposite slopes of the canyon are separated by 50-100 m at the bottom, have identical geology and soil types, but have different vegetation. The "African" slope is more stressful for many mesic organisms [27-33]. The microclimatic differences cause strong local biodiversity differentiation at all developmental levels (sequences, genes, genomes, populations, species, ecosystems, and biota), and are accompanied by interslope differences in the specie's richness and abundance [27-31].

Twenty four species belonging to different taxonomic groups were measured [11-13]. The results of these studies are summarized and show (Table 1) that fluctuating asymmetry is negatively correlated with abundance; 17 of the 23 species (74%) displayed higher fluctuating asymmetry on the slope where they were less abundant (p = 0.0347 in binomial test). On the other hand, only 13 of the 23 species showed higher fluctuating asymmetry on the "African" slope (p = 0.54). Our results additionally suggest that the "African" slope is extremely stressful only for species that are on the margins of their adaptive zones. Likewise, the "European" slope is extremely stressful only for species that are on the margins of their different adaptive zones. In these cases, differences in body size represent adaptation rather than the current stress effect.

These results show that a broad approach, encompassing many species (using the same methods), may allow researchers

Table 1: Variation in size and fluctuating asymmetry in the studied taxonomic group.

Taxonomic group	Number of studied species	Percentage of species with bigger sizes on the "European Slope"	Percentage of species displaying a negative correlation between FA and abundance
Vascular plants	12	100	72.7
Soil microfungi	5	60	80
Land-snails	6	60	60
Beetles	1	100	100
Overall Significance		$P*$ = 0.0026	$P*$ = 0.0347

*In binomial test

to make generalizations regarding the ability of fluctuating asymmetry to serve as an indicator of stress, and decrease the effect of variability among studies. This is according to Zakharov [34], who suggested a biotest approach, which suggests that the fluctuating asymmetry of several species should be integrated for the study of environmental stress. Graham [35] suggested using meta-analysis when studying several species. However, this approach has been rarely used. Most studies still examine just a single species at a time, and the results are always ambiguous and non-generalizable [35].

Computational modeling of asymmetry of shape using Continuous Symmetry Measurements (CSM)

Three types of objects for quantifying metric asymmetry are given in Figure 2. Landmark methods give the appropriate attention to consistent and partially consistent objects, and continuous symmetry measures extend that attention to inconsistent objects. Consistently symmetrical objects have a consistent topology of specific landmarks that display some form of symmetry. The position of the corresponding landmarks, and the distances among them, may vary (Figure 2A), but their number is maintained. Inconsistent objects have no homologous landmarks, no consistent topology, no quantitative consistency, and sometimes no matching points (Figure 2C).

Landmark methods use developmentally homologous points (i.e., landmarks) for asymmetry analysis, and they represent an advancement of the conventional measurement of distance. Continuous Symmetry Measures (CSM) [10] treat symmetry as a continuous feature rather than a binary feature (i.e., whether it exists or not), and it involves the amount of "effort" required to transform a given shape (composed of orbits) into a symmetric shape. Continuous symmetry measures are an advancement over landmark methods [26] because they can measure deviations from symmetry of objects that have variable structural elements. Hence, they encompass the landmark methods.

Modeling leaf asymmetry using continuous symmetry measure: The leaf vein's bifurcation structure is an example of a structure that cannot be quantified using landmark methods. Typically, the middle and secondary veins of leaves display planar, tree-like (i.e., bifurcating) geometry. The general

Figure 1: The opposing slopes of "Evolution Canyon" I, Lower Nahal Oren, Mt. Carmel. The xeric "African" slope is on the right, and the music "European" slope is on the left [31].

layout of the veins consists of a central mid-vein, the symmetry axis from which secondary veins bifurcate on both sides. Individual leaves may vary in the number of secondary veins, their bifurcation points along the mid-vein, their lengths, and their angles. Since no geometric or structural consistency can be assumed, we propose to define matching points based on a biological-specific physiological mechanism, namely the Leaf Venation Hypothesis [36,37] and on the concept of minimum energy [38] (Figure 3).

Milner, et al. [39] developed a way to quantify the amount of asymmetry of one-level bifurcation structure of leaf veins. Since, usually the asymmetry developmentally originates during the early stages of leaf growth; we attempted to quantify the asymmetry introduced during the developmental stages of leaf growth based on the described growth model (Figure 4). Although many factors and chemical substances are involved in the growth process, the model was simplified by considering only the effects on the vein structure of the asymmetries in concentration of auxin in the leaf.

In this approach, the bifurcating structure is viewed as a collection of points interconnected by segments (Figure 5A). The approach requires matching pairs of points to be deformed into symmetric pairs. In the case of our bifurcating structures, this pairing of points reduces to pairing of secondary veins. Figure 5B shows an example where points on paired veins have been matched (point Pk matches point Qk). In the case of a "missing" secondary vein, an insertion of a new vein of zero length is required, which is marked as two endpoints located at the bifurcation point.

The CSM, as shown on bifurcating structures, enables us to study structures that landmarks are not capable of, in a way that is similar to the ability of landmarks methods to study structures that linear measurements are not capable of. The CSM, however, requires identification of the landmarks of the studied structure. Gandhi, et al. [40] used methodologies from information theory in order to find the most appropriate type of symmetry, and to quantify the degree of symmetry using automatic detection of the studied object.
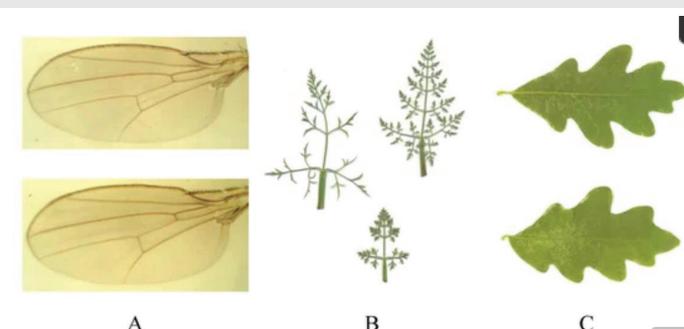

Figure 3: Schematic diagrams showing gradual changes in sites (blue spot locations) and concentrations (blue symbol sizes) of free indole-3-acetic acid production during leaf development in Arabidopsis. Arrows mark the sites with the highest level of primary free auxin production, which is located at the leaf margin in each developmental stage (A−D); arrowheads show the location of low free auxin production in the lamina (D−E). The ontogeny of midvein and secondary vascular bundles is illustrated by broken red lines, while marginal and minor veins are not shown [38].
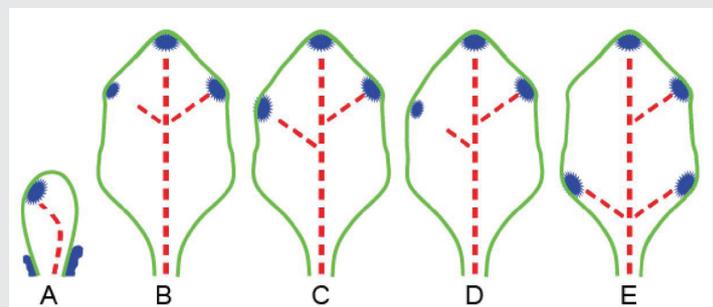
Figure 4: Schematic diagrams showing secondary veins structures (broken red line) and suggested active free- auxin center location (blue spot location) and concentration (blue spot size). (A) Asymmetry in the auxin concentration in the stipules and in the tip auxin center location. (B) Unequal primary- free auxin production (e.g., concentration) in the upper lobes, which induces asymmetry in the length of the secondary veins. (C) Misalignment of auxin concentration sites, while maintaining equality of concentration magnitude, which induces asymmetric bifurcation points along the main vein. (D) Unequal location of auxin production site, together with unequal auxin concentration, induces asymmetry in the secondary veins' length and asymmetric bifurcation points along the main vein. (E) Missing partnering secondary veins due to low auxin concentration. Paired secondary veins may or may not exist in lower lobes [39].
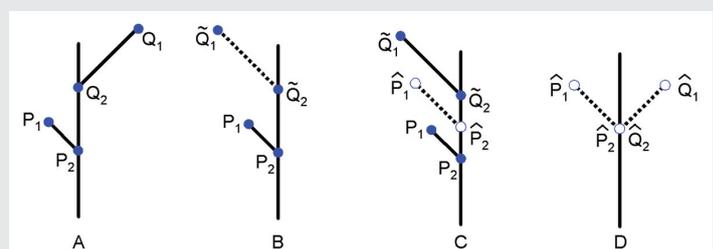
Figure 5: Computing the CSM using the folding-unfolding method applied to 2 paired secondary veins, each represented by 2 points. (A) Original bifurcating structure with matching points marked. (B) Fold − Vein Q is reflected across the symmetry axis obtaining the folded points $\tilde{Q}_1$ and $\tilde{Q}_2$. (C) Average − The folded points are averaged with their matching points obtaining the points $\hat{P}_1$ and $\hat{P}_2$. (D) Unfold − The average points are reflected back across the symmetry axis obtaining the unfolded points $\hat{Q}_1$ and $\hat{Q}_2$. The CSM value is the average distance squared between the original points and the corresponding unfolded points $\frac{1}{4}\left[\left(P_1 - \hat{P}_1\right)^2 + \left(P_2 - \hat{P}_2\right)^2 + \left(Q_1 - \hat{Q}_1\right)^2 + \left(Q_2 - \hat{Q}_2\right)^2\right]$ [39].

Figure 2: Three types of objects for quantifying metric asymmetry. A. Structures having consistent topology and number of landmarks (Drosophila melanogaster wings). B. Structures having consistent topology, but a varying number of corresponding landmarks among specimens (the secondary veins of Daucus carota leaves). C. Variable structures having no consistent topology, no quantitative consistency, and sometimes no matching points (lobes and sinuses on the leaves of *Quercus Alba*) [26].
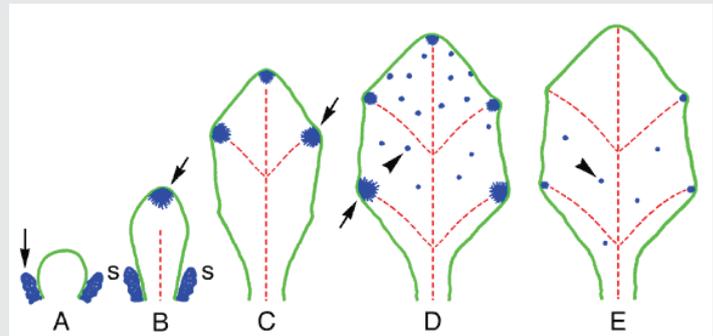
Asymmetry as neurophysiological bioindicator

One of the early symptoms of Neurological Disorders, and more specifically neurodegenerative disorders, is directional asymmetry of the face or the body of the patient. For example, Parkinson's Disease (PD) and Cerebrovascular Accident (CVA-Stroke) asymmetrically affect the oro-facial musculature with major impairments to speech, swallowing, and oro-motor abilities, as well as expression of emotions [41]. A timely and accurate assessment of oro-facial impairments can contribute to the overall disease diagnosis and lead to early interventions and improved quality of life [42-44].

There are many studies that quantify the body-face morphologies of these asymmetric diseases and disorders. For example, Chang, et al. [45] proposed a facial stroke recognition system, which showed that the proposed system can accurately and effectively distinguish stroke from non-stroke images. Bandini, et al. [46] suggested video-based facial tracking systems that could assist with early diagnosis and progress monitoring of bulbar ALS disease progression. Asymmetrical features can be used also on cortical brain recordings (EEG) to classify even very subtle neurological phenomena such as Dyslexia and ADHD [47]. Symmetry can be also expressed by synchrony of the brain areas [48,49]. Asymmetrical behavior can be spotted also in most fine motor movements such as finger tapping [50,51].

In another study, we quantified the level of stroke rehabilitation based on the Fugl-Meyer Assessment (FMA) [52,53]. This test involves the patient performing specific motor actions. A physician or skilled medical professional rates the performance on the FMA scale, and a subjective score is derived. A novel multi-camera tracking system was applied to evaluate the motor movement of stroke patients (Figure 6).

The subjects performed the Fugl-Meyer assessment, and the FMA scores for the patients and the healthy subjects were estimated. An analysis application was developed for extracting measurements from the tracked body skeleton recordings, as shown in Figure 6, and these measurements were then used to detect correlations with the physician's diagnosis.

We showed very high classification rates between stroke patients and healthy subjects using our Fugl-Meyer tracking and analysis system [52]. However, the results also showed that classification that used the asymmetry measure yielded inferior results when compared to the other data sets. This, and the fact that the classifications were run on data from both the affected and healthy body sides, implies that both the stroke-affected side and the subject's healthy side provided distinguishing features, which enabled the separation of patients from healthy subjects.

The rationale behind developing these AI measures is that the state-of-the-art clinical methods are usually subjective and variant to the clinician who performs the evaluation of the existence and progress of the disease. So, there is a need for automatic, non-biased tools.

Currently, the use of artificial intelligence and stroke diagnosis is being coupled for life-saving applications such as the start-up company CVAid Medical, which was co-founded by Doctor Shmuel Raz, a co-author of this review. CVAid Medical was established to perform stroke diagnosis and management by using a smartphone application along with a battery of computer vision and machine learning tools. The CVAid facial recognition system showed an accuracy of 87% in stroke symptom detection, sensitivity 95%, specificity 80%, false negative 5%, false positive 20% [54].

Acknowledgement

References

1. Valen L. Van A Study of Fluctuating Asymmetry. Evolution (N. Y). 1962, 16, 125, doi:10.2307/2406192.

2. Soule M. Phenetics of Natural Populations. II. Asymmetry and Evolution in a Lizard. Am Nat. 1967. 101:141-160. doi:10.1086/282480.

3. Mather K. Genetical Control of Stability in Development. Heredity (Edinb). 1953; 7: 297–336.

4. Danforth CH. Resemblance and Difference in Twins: Twins That Look and Act Alike Attract Attention First, While Dissimilar Ones Are Apt to Be Overlooked. J Hered 1919; 10: 399-409. doi:10.1093/oxfordjournals.jhered.a101956.

5. Sumner FB, Huestis RR. Bilateral Asymmetry and Its Relation To Certain Problems of Genetics. Genetics. 1921; 6: 586–586. doi:10.1093/genetics/6.6.586.

6. Graham JH, Freeman DC, Emlen JM. Developmental Stability: A Sensitive Indicator of Populations under Stress. ASTM Spec Tech Publ. 1993; 1179: 136-158, doi:10.1520/stp19239s.

7. Klingenberg CP, Mcintyre GS. Geometric Morphometrics of Developmental Instability: Analyzing Patterns of Fluctuating Asymmetry with Procrustes Methods. Evolution (N.Y). 1998; 52: 1363-1375. doi:10.1111/j.1558-5646.1998.tb02018.x.

8. Freeman DC, Graham JH, Emlen JM, Tracy MA, Hough RA, Alados CL, Escos J. Plant Developmental Instability: New Measures, Applications and Regulation. 2003.

9. Milner D, Hel-Or H, Keren D, Raz S, Nevo E. Analyzing Symmetry in Biological Systems. In Proceedings of the IEEE International Conference on Image Processing 2005. 2005; 1: 1-361.
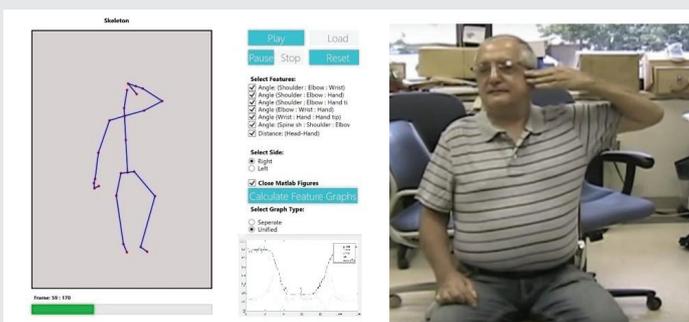
Figure 6: [52] Analysis of the Fugl-Meyer hand salute test.

10. Zabrodsky H, Peleg S, Avnir D. Symmetry as a Continuous Feature. IEEE Trans Pattern Anal Mach Intell. 1995; 17: 1154–1166.

11. Raz S, Schwartz NP, Mienis HK, Nevo E, Graham JH. Fluctuating helical asymmetry and morphology of snails (Gastropoda) in divergent microhabitats at 'Evolution Canyons I and II,' Israel. PLoS One. 2012;7(7):e41840. doi: 10.1371/journal.pone.0041840. Epub 2012 Jul 26. PMID: 22848631; PMCID: PMC3406068.

12. Raz S, Graham JH, Cohen A, de Bivort BL, Grishkan I, Nevo E. Growth and asymmetry of soil microfungal colonies from "Evolution Canyon," Lower Nahal Oren, Mount Carmel, Israel. PLoS One. 2012;7(4):e34689. doi: 10.1371/journal.pone.0034689. Epub 2012 Apr 16. PMID: 22523554; PMCID: PMC3327715.

13. Raz S, Graham JH, Hel-Or H, Pavlíček T, Nevo E. Developmental Instability of Vascular Plants in Contrasting Microclimates at "Evolution Canyon." Biol J Linn Soc. 2011; 102: 786-797. doi:10.1111/j.1095-8312.2011.01615.x.

14. Graham JH, Felley JD. GENOMIC COADAPTATION AND DEVELOPMENTAL STABILITY WITHIN INTROGRESSED POPULATIONS OF ENNEACANTHUS GLORIOSUS AND E. OBESUS (PISCES, CENTRARCHIDAE). Evolution. 1985 Jan;39(1):104-114. doi: 10.1111/j.1558-5646.1985.tb04083.x. PMID: 28563632.

15. Sangster TA, Salathia N, Undurraga S, Milo R, Schellenberg K, Lindquist S, Queitsch C. HSP90 affects the expression of genetic variation and developmental stability in quantitative traits. Proc Natl Acad Sci U S A. 2008 Feb 26;105(8):2963-8. doi: 10.1073/pnas.0712200105. Epub 2008 Feb 19. PMID: 18287065; PMCID: PMC2268568.

16. Debat V, Milton CC, Rutherford S, Klingenberg CP, Hoffmann AA. Hsp90 and the quantitative variation of wing shape in Drosophila melanogaster. Evolution. 2006 Dec;60(12):2529-38. PMID: 17263114.

17. Midgley GF, Wand SJE, Musil CF. Repeated Exposure to Enhanced UV-B Radiation in Successive Generations Increases Developmental Instability (Leaf Fluctuating Asymmetry) in a Desert Annual. Plant Cell Environ. 1998; 21: 437–442, doi:10.1046/j.1365-3040.1998.00274.x.

18. Hosken DJ, Blanckenhorn WU, Ward PI. Developmental Stability in Yellow Dung Flies (Scathophaga Stercoraria): Fluctuating Asymmetry, Heterozygosity and Environmental Stress. J Evol Biol. 2000; 13: 919–926.

19. Milton GW, Sawicki AT. Theory of Composites. Cambridge Monographs on Applied and Computational Mathematics. Appl Mech Rev. 2003; 56: B27–B28.

20. Leary RF, Allendorf FW. Fluctuating asymmetry as an indicator of stress: Implications for conservation biology. Trends Ecol Evol. 1989 Jul;4(7):214-7. doi: 10.1016/0169-5347(89)90077-3. PMID: 21227354.

21. Møller AP, Swaddle JP. Asymmetry, Developmental Stability and Evolution; Oxford University Press, UK, 1997.

22. Leamy LJ, Klingenberg CP. The Genetics and Evolution of Fluctuating Asymmetry. Annu Rev Ecol Evol Syst. 2005; 36: 1-21. doi:10.1146/annurev.ecolsys.36.102003.152640.

23. Hoffman AA, Woods RE. Associating Environmental Stress with Developmental Stability: Problems and Patterns. Dev Instab causes consequences. 2003; 387-401.

24. Leung B, Forbes MR. Fluctuating Asymmetry in Relation to Stress and Fitness: Effects of Trait Type as Revealed by Meta-Analysis. Ecoscience. 1996; 3: 400–406, doi:10.1080/11956860.1996.11682357.

25. Raz S. Exploring and Modeling Fluctuating Asymmetry and Morphology in Diverese Taxa under Sharp Microclimatic Divegence at the "Evolution Canyons" Microsites,"Mount Carmel" and Upper Galilee; University of Haifa (Israel). 2011.

26. Graham JH, Raz S, Hel-Or H, Nevo E. Fluctuating Asymmetry: Methods, Theory, and Applications. Symmetry (Basel). 2010; 2: 466–540.

27. Nevo E. Asian, African and European Biota Meet at "Evolution Canyon" Israel: Local Tests of Global Biodiversity and Genetic Diversity Patterns. Proc R Soc B Biol Sci. 1995; 262: 149–155, doi:10.1098/rspb.1995.0189.

28. Nevo E. Evolution in action across phylogeny caused by microclimatic stresses at "Evolution Canyon". Theor Popul Biol. 1997 Dec;52(3):231-43. doi: 10.1006/tpbi.1997.1330. PMID: 9466964.

29. Nevo E. Evolution of genome-phenome diversity under environmental stress. Proc Natl Acad Sci U S A. 2001 May 22;98(11):6233-40. doi: 10.1073/pnas.101109298. PMID: 11371642; PMCID: PMC33451.

30. Nevo E. Evolution Canyon: A Microcosm of Life's Evolution Focusing on Adaptation and Speciation. Isr J Ecol Evol. 2006; 52: 501–506. doi:10.1560/ijee_52_3-4_485.

31. Nevo E. Evolution in Action across Life at "Evolution Canyons", Israel. Trends Evol Biol. 2009; 1: 12–34, doi:10.4081/eb.2009.e3.

32. Nevo E, Raz S, Beiles A. Biodiversity of Reptiles at "Evolution Canyon", Lower Nahal Oren, Mount Carmel, Israel. Isr J Zool. 1996; 42: 395-402.

33. Raz S, Retzkin S, Pavlíček T, Hoffman A, Kimchi H, Zehavi D, Beiles A, Nevo E. Scorpion Biodiversity and Interslope Divergence at "Evolution Canyon", Lower Nahal Oren Microsite, Mt. Carmel, Israel. PLoS One. 2009; 4: e5214, doi:10.1371/journal.pone.0005214.

34. Zakharov VM. Biotest: A New Integrated Biological Approach for Assessing the Condition of Natural Environments. 1993.

35. Graham JH. Fluctuating Asymmetry and Developmental Instability, a Guide to Best Practice. Symmetry (Basel). 2021; 13: 1-8. doi:10.3390/sym13010009.

36. Aloni R. Foliar and Axial Aspects of Vascular Differentiation: Hypotheses and Evidence. J Plant Growth Regul. 2001; 20: 22–34, doi:10.1007/s003440010001.

37. Aloni R, Schwalm K, Langhans M, Ullrich CI. Gradual Shifts in Sites of Free-Auxin Production during Leaf-Primordium Development and Their Role in Vascular Differentiation and Leaf Morphogenesis in Arabidopsis. Planta. 2003; 216: 841–853. doi:10.1007/s00425-002-0937-8.

38. Ullrich CI, Aloni R. Vascularization is a general requirement for growth of plant and animal tumours. J Exp Bot. 2000 Dec;51(353):1951-60. doi: 10.1093/jexbot/51.353.1951. PMID: 11141169.

39. Milner D, Raz S, Hel-Or H, Keren D, Nevo E. A New Measure of Symmetry and Its Application to Classification of Bifurcating Structures. Pattern Recognit. 2007; 40:0 2237–2250. doi:10.1016/j.patcog.2006.12.008.

40. Gandhi S, Klein J, Robertson AJ, Peña-Hernández MA, Lin MJ, Roychoudhury P, Lu P, Fournier J, Ferguson D, Mohamed Bakhash SAK, Catherine Muenker M, Srivathsan A, Wunder EA Jr, Kerantzas N, Wang W, Lindenbach B, Pyle A, Wilen CB, Ogbuagu O, Greninger AL, Iwasaki A, Schulz WL, Ko AI. De novo emergence of a remdesivir resistance mutation during treatment of persistent SARS-CoV-2 infection in an immunocompromised patient: a case report. Nat Commun. 2022 Mar 17;13(1):1547. doi: 10.1038/s41467-022-29104-y. PMID: 35301314; PMCID: PMC8930970.

41. Frid A, Manevitz LM, Mosafi O. Kohonen-Based Topological Clustering as an Amplifier for Multi-Class Classification for Parkinson's Disease. In Proceedings of the 2018 IEEE International Conference on the Science of Electrical Engineering in Israel (ICSEE). 2018; 1–5.

42. Bologna M, Fabbrini G, Marsili L, Defazio G, Thompson PD, Berardelli A. Facial bradykinesia. J Neurol Neurosurg Psychiatry. 2013 Jun;84(6):681-5. doi: 10.1136/jnnp-2012-303993. Epub 2012 Dec 12. PMID: 23236012.

43. Flowers HL, Silver FL, Fang J, Rochon E, Martino R. The incidence, co-occurrence, and predictors of dysphagia, dysarthria, and aphasia after first-ever acute ischemic stroke. J Commun Disord. 2013 May-Jun;46(3):238-48. doi: 10.1016/j.jcomdis.2013.04.001. Epub 2013 Apr 12. PMID: 23642855.

44. Langmore SE, Lehman ME. Physiologic deficits in the orofacial system underlying dysarthria in amyotrophic lateral sclerosis. J Speech Hear Res. 1994 Feb;37(1):28-37. doi: 10.1044/jshr.3701.28. PMID: 8170127.

45. Chang CY, Cheng MJ, Ma MHM. Application of Machine Learning for Facial Stroke Detection. In Proceedings of the International Conference on Digital Signal Processing. DSP 2019; 2018: 1–5.

46. Bandini A, Green JR, Zinman L, Yunusova Y. Classification of Bulbar ALS from Kinematic Features of the Jaw and Lips: Towards Computer-Mediated Assessment. In Proceedings of the Proceedings of the Annual Conference of the International Speech Communication Association. Interspeech. 2017; 1819–1823.

47. Frid A, Manevitz LM. Features and Machine Learning for Correlating and Classifying between Brain Areas and Dyslexia. arXiv Prepr. arXiv1812.10622 2018.

48. Frid A, Breznitz Z. Processing Information during a Lexical Decision Task as an Indication of Brain Region Synchronization: Differences between Dyslexic and Regular Readers. In Proceedings of the Journal of Molecular Neuroscience. 2014; 53: S47-S48.

49. Frid A, Safra EJ, Hazan H, Lokey LL, Hilu D, Manevitz L, Ramig LO, Sapir S. Computational Diagnosis of Parkinson's Disease Directly from Natural Speech Using Machine Learning Techniques. In Proceedings of the 2014 IEEE International Conference on Software Science, Technology and Engineering. 2014; 50–53.

50. Frid A, Lavner Y, Rabinowitz I. Analysis of Finger Tapping Parameters in People with ADHD. In Proceedings of the 2012 IEEE 27th Convention of Electrical and Electronics Engineers in Israel. 2012; 1-4.

51. Dror B, Yanai E, Frid A, Peleg N, Goldenthal N, Schlesinger I, Hel-Or H, Raz S. Automatic Assessment of Parkinson's Disease from Natural Hands Movements Using 3D Depth Sensor. In Proceedings of the 2014 IEEE 28th Convention of Electrical and Electronics Engineers in Israel, IEEEI 2014; 2014; 1–5.

52. Eichler, N.; Hel-Or, H.; Shimshoni, I.; Itah, D.; Gross, B.; Raz, S. 3D Motion Capture System for Assessing Patient Motion during Fugl-Meyer Stroke Rehabilitation Testing. IET Comput Vis. 2018; 12: 963-975. doi:10.1049/iet-cvi.2018.5274.

53. Fugl-Meyer AR, Jaasko L, Leiman I, Olson S, Steglind S. The Post-Stroke Hemiplegic: A Method for Evaluation of Physical Performance. Scand J Rehab Med 1975. 61: 13–32.

54. Ribo M, Reznik A, Ciolli L, Ohanyan S, Brancaleoni L, Sanhueza D, Sivan-Hoffmann R. Artificial Intelligence-Based Application to Detect and Quantify Stroke Symptoms. Stroke. 2020; 51: A94-A94.